INSTITUTE OF PHYSICS PUBLISHING PHYSIOLOGICAL MEASUREMENT

Physiol. Meas. **25** (2004) 1511–1522 PII: S0967-3334(04)81668-X

Miniaturization of a biomedical gas sensor

Peyman Mirtaheri[1,2,3], Tore Omtveit[4], Thomas Klotzbuecher[5], Sverre Grimnes[2,3], Ørjan G Martinsen[2] and Tor Inge Tønnessen[1,6]

[1] The Interventional Center, Rikshospitalet University Hospital, 0027 Oslo, Norway
[2] Department of Physics, University of Oslo, PB 1048 Blindern, Norway
[3] Department of Clinical Engineering, Rikshospitalet University Hospital, Oslo, Norway
[4] Alertis Medical AS, Oslo, Norway
[5] Institut für Mikrotechnik Mainz GmbH, Optics Department, Mainz, Germany
[6] Department of Anesthesiology, Rikshospitalet University Hospital, Oslo, Norway

Received 3 June 2004, accepted for publication 12 October 2004
Published 10 November 2004
Online at stacks.iop.org/PM/25/1511
doi:10.1088/0967-3334/25/6/015

Abstract

In a previous study, we concluded that a conductivity based PCO_2 sensor is an attractive solution for early detection of ischemia and presented two design geometries. For organ surface measurements, the planar design was suitable but it was difficult to insert the sensor into the tissue. A cylindrical design solution was favored for insertion due to the large membrane contact area and easy placement in a medical catheter. Since the previous cylindrical prototype was large and could damage the tissue, a more miniaturized sensor was needed. In the current paper, we present a miniaturized sensor with an outer diameter of 1 mm. The applied technology for manufacturing the sensor was a combination of mechanical turning, excimer laser drilling and conventional molding technique. The materials applied were PEEK (polyetherether ketone), PI (polyimide) with gold layers and polysiloxane. The membrane had to be gas permeable while acting as a barrier for ion transport, and was made of polysiloxane and had a thickness of 100–150 μm. The miniaturized sensor was tested for calibration, response time, drifting and pressure sensitivity. The results show that the miniaturized PCO_2 sensor is capable of rapid and stable measurements both *in vitro* and *ex vivo*. The result from this study will be applied for the industrial manufacturing of such a biomedical sensor as a clinical product.

Keywords: conductivity, ischemia, miniaturization, PCO_2 sensor

1. Introduction

Ischemia can be detected early by measuring the partial pressure of carbon dioxide (PCO_2) levels in the organs (Kvarstein *et al* 2003, 2004, Tønnessen 1997, Tønnessen and Kvarstein 1996). When the demand for blood (oxygen) by an organ exceeds the supply, an ischemic condition will occur. The cells will switch into anaerobic metabolism and generate large amounts of lactic acid. In order to maintain normal intracellular pH value, the acid produced is buffered by proteins, phosphates and bicarbonates. The buffering of protons by bicarbonates will produce large amounts of carbon dioxide. Consequently, measuring the PCO_2 in the tissue can be applied as a marker for early detection of ischemia and a miniaturized PCO_2 sensor, which damages the tissue minimally, and can be applied as an ischemia detector.

As reported by Mirtaheri *et al* (2004), a conductivity based PCO_2 sensor was developed and two design prototypes were compared with each other. The conductivity-based PCO_2 sensor consisted of a closed chamber filled with de-ionized water, a gas permeable membrane serving as the interface between the water and the tissue and two electrodes. Since the reaction of CO_2 and water forms carbonic acid, which further dissociates into protons and bicarbonate ions, it is possible to measure the concentration of the produced ions by using a conductometric measuring technique. The concentration of protons and bicarbonate is proportional to the square root function of concentration of CO_2. PCO_2 is proportional to the concentration of CO_2 as expressed by Henry's law (Nunn 1993). Thus, the relation between the conductivity and PCO_2 is

$$G_e = \Psi \cdot \left(\sigma_0 + m \cdot (PCO_2)^{1/2}\right)$$

where the constant Ψ[m] is a geometrical factor and is equal to the area divided by the length of the measuring cell, σ_0 [S m^{-1}] is the conductivity when the PCO_2 is 0 kPa, m is a constant and equal to $(\Lambda^\circ_{H+} + \Lambda^\circ_{HCO3^-})\,(K \cdot K_H)^{1/2}$, where Λ°[m^2 (Ω mol)$^{-1}$] is the molar conductivity of ions at infinite dilution, K is the equilibrium constant and K_H [mol (l kPa)$^{-1}$] is Henry's constant, respectively. We assume that the ion concentrations are sufficiently small so that the equivalent conductivities at infinite dilution (Λ°) are applied, and consequently the activity coefficient (ϑ_i) of the proton and bicarbonate ions approaches unity (Himpler *et al* 1978). Henry's constant K_H is dependent on the intermolecular forces between the solvent and the gas, and temperature (Nunn 1993).

The value of $\Psi \cdot \sigma_0$ is the baseline of the sensor and is dependent on the purity of the de-ionized water applied to fill the sensor, and the volume of the measurement cell. Assuming that the volume of the measurement cell is constant, a change of the baseline value would be due to the ion contamination, which increases the conductivity of the water σ_0.

The sources of errors for a conductivity based PCO_2 measurement with an unchanged geometry cell volume are related to the electrode polarization effect, the stray capacitance noise interferences, ion intrusion into the measuring chamber and temperature. The electrode polarization contribution decreases by increasing frequency (Schwan 1968). With an increased frequency, however, the influence of the stray capacitance noise will be larger (Grimnes and Martinsen 2000). Although the electrode polarization contribution could be avoided by using the four-electrodes measurement technique (Schwan and Ferris 1963), the drawback would be high stray capacitance influence and a more complex design. The membrane has to be gas permeable, but no ion should get through the membrane in order to avoid drifting. Finally, the temperature is not only affecting the partial pressure of the carbon dioxide but also the conductivity. The measured values have to be corrected for the temperature variations.

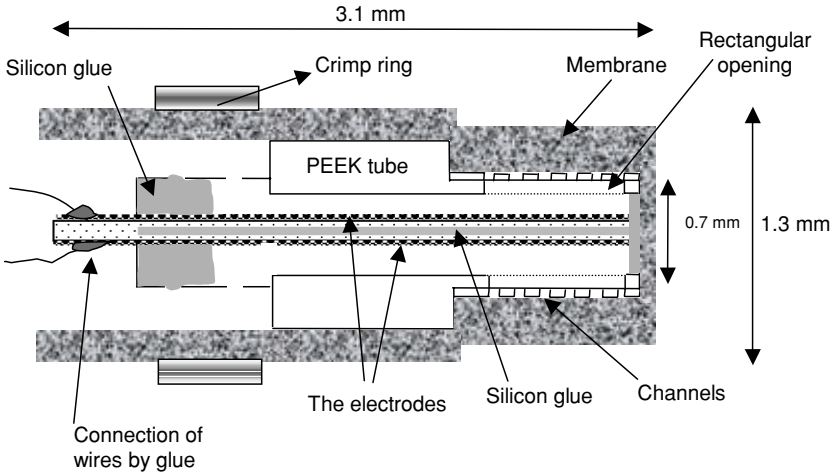

Figure 1. Drawing of the PCO_2 sensor assembled with three components, PEEK cylinder, polysiloxane membrane and the electrode assembly with wires glued at the rear end.

The purpose of the bridge channel geometry was to minimize the contribution of the electrode polarization effect with moderately low frequencies (Mirtaheri *et al* 2004).

The cylindrically shaped sensor, described in the previous study, was too large and had to be redesigned for miniaturization. With a miniaturized sensor, it will be easier to place the sensor into the tissue with minimal disturbances of the microcirculation to avoid damage to the vessels.

The main goal of this study was to miniaturize the conductivity based PCO_2 sensor. The cylindrically shaped sensor was redesigned with respect to miniaturization ratio aspects and easy production capability with fewer components. The performance of the manufactured sensor was tested for calibration, drift, temperature and total pressure. The results of this paper may be used for manufacturing a miniaturized PCO_2 sensor for clinical trials.

2. Materials and methods

2.1. Design

The new sensor design presented in this paper is similar to the macro prototype of the cylindrically shaped sensor, with the exception of parallel multiple bridge channels and the placement of the electrodes.

The current sensor consists of three main parts, a PEEK (polyetheretherketone) hollow cylinder with six circular channels interrupted by two rectangular openings, a polyimide foil coated with gold layers on the bottom and top side and a polysiloxane membrane (figure 1).

2.1.1. The PEEK tube. A PEEK rod material of thickness 10 mm was clamped onto a turning machine and turned down to a diameter of 0.7 mm at front and back end and 1mm for the middle part. PEEK was chosen since it was easy to turn in small dimensions. Six parallel rings with the width and depth of 0.1 mm $\times$ 0.3 mm were turned in the PEEK rod. The rectangular holes were fabricated by excimer laser machining (figures 2(a) and 3). The PEEK tube does not only serve as a mechanical stabilization of the soft membrane but also as the protection for the gold layers. In addition, the small channels (figures 1 and 3) were designed to support

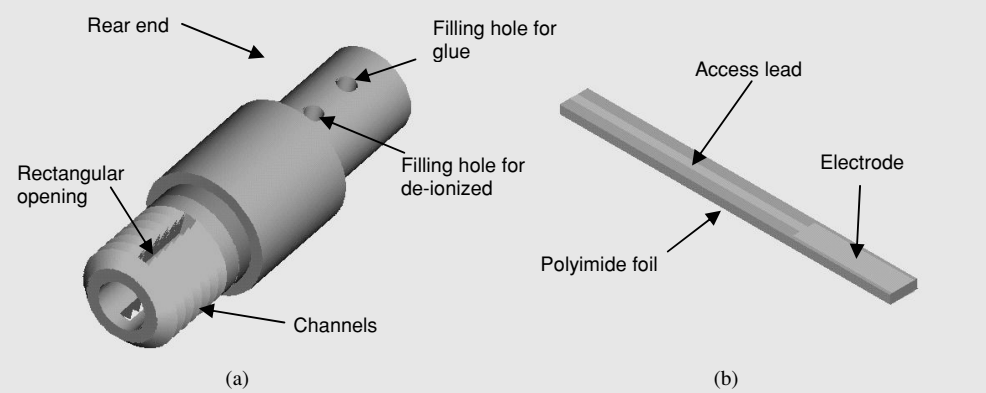

Figure 2. The drawings of sensor inner parts without the membrane, (a) PEEK cylinder and the circular ring channels, (b) electrode assembly with polyimide foil covered with gold layer after laser patterning.

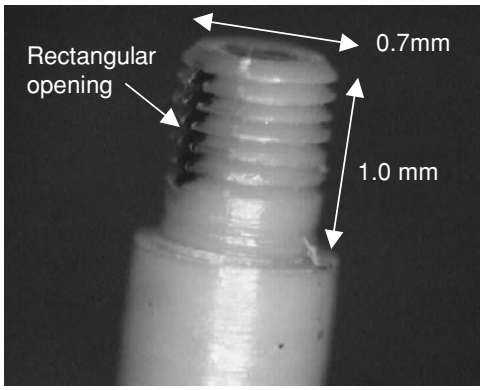

Figure 3. Photograph of the sensor inner part before the assembly of the polyimide foil. The inner part is made of a turned PEEK rod with rectangular openings drilled by the excimer laser ablation.

the membrane and achieve less pressure sensitivity. The PEEK tube had two rectangular holes on each side, which allowed the penetration of the current field from the top to the bottom electrodes. Beneath these rectangular holes, there are two water reservoirs, which keep the channels filled with water.

Since the channels are interrupted by the rectangular holes, the total number of parallel channels is actually 12 . The cross section for each of the 12 parallel channels and the length were about 0.1 mm $\times$ 0.3 mm and 0.6 mm, corresponding to a geometry constant of $\psi = 6 \times 10^{-3}$ m.

2.1.2. Electrode assembly. The material applied for supporting the electrodes should have a low absorption coefficient since the water absorbed in the material may cause leakage currents between the electrodes. We chose therefore polyimide as the support material since it had a very low water absorption coefficient and also was a suitable material for adhesion of metal plating.

We could choose platinum, silver or gold for the electrode material. However, gold was chosen since it is known as a stable material and easy to work with, in addition to its low ratio aspect of electrode polarization impedance versus bulk resistance of the electrolyte

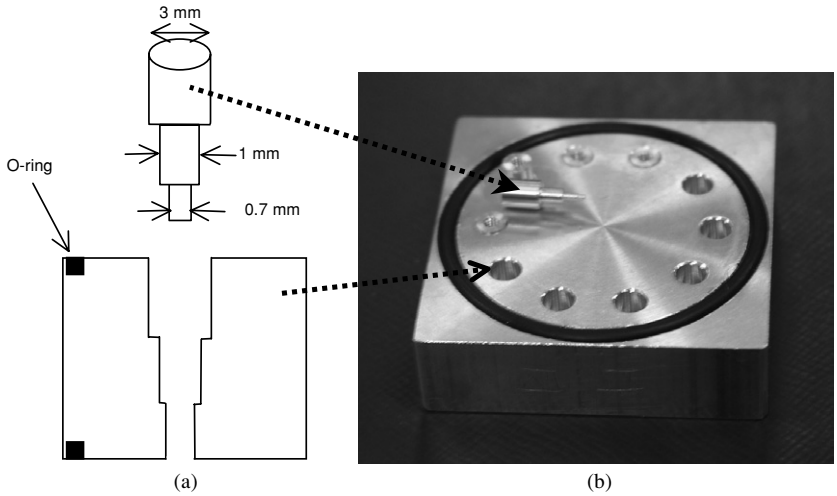

Figure 4. (a) The side view drawing of the molding tool and (b) the actual photograph of the molding tool and the pins. The O-ring makes a sealing between the top and bottom plates during the molding.

(unpublished data). The electrode assembly was fabricated by coating a 125 μm thick polyimide foil (PI) with a 100 nm thick gold layer (figure 1(b)). The coating with gold was done on both sides of the PI substrate. After the coating process was done, the electrode area was formed by the excimer laser ablation as shown in figure 2(b).

2.1.3. Molding the membrane. PTFE (polytetrafluoroethylene) as a membrane material is very difficult to work with since it is hard to glue and process. Other materials that have hydrophobic properties as PTFE are silicone rubber and polyethylene. A silicone rubber material such as polysiloxane was chosen since it is easier to apply in molding process. In addition, CO_2 gas can diffuse much faster in polysiloxane (Arquint 1994). The disadvantage of polysiloxane is its low mechanical robustness, which is very much dependent on its manufacturing process.

Molding the silicone rubber in such a small dimension is a rather difficult manufacturing process. Since the membrane had connective areas covering the front end, middle part and back end of the sensor, the material should have large tear strength. A two-component polysiloxane material (Elastosil 402, Wacker chemical) was used. According to the manufacturer, different strength is achieved by varied temperature and pressure inside the mold.

For the casting of the membrane, a mold insert tool was designed and fabricated (figure 4(a)). To make enough membranes simultaneously, we fabricated a brass mold with ten cavities (figure 4(b)). The front end of each pin was 0.7 mm diameter with a length of 1 mm then the diameter increases to 1 mm and finally to 3 mm. The last part of the pin was acting as a guide for the 0.7 mm tip. The mold was pressed between two plates. A top plate pressed the pins inside the cavities while a bottom plate avoids the polysiloxane to run out of the cavities. By decreasing the distance between the top and bottom plates, it is possible to achieve a higher pressure inside the cavity. According to the manufacturer, a high tearing strength for the polysiloxane membrane would be achieved by choosing a working temperature of 150 °C, and a pressure of about 2.0 atmospheres. The mold was kept in the oven for about 1 h at 150 °C at a double atmospheric pressure and then for 5 h at 70 °C for the vulcanization and

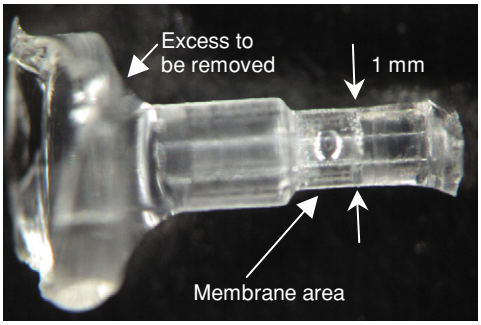

Figure 5. Picture of the de-molded membrane before the molding excess was removed.

after vulcanization processes, respectively. After the vulcanization processes, the membranes were de-molded by taking the pins carefully out of the mold cavities, and then by a vacuuming procedure the membranes were separated from the pins. The membrane after demoulding looked as in figure 5 and the excess parts due to the molding tool were removed by a surgical scalpel. The thickness of the membrane wall was then measured by an optical shadowgraph (Nikon, 5A) and those that were in the range of 100–150 μm were selected.

2.1.4. Assembly of the parts. According to the equation introduced in the introduction section, the baseline of the sensor is $\Psi \cdot \sigma_0$, and it would be affected by the ion contamination in the sensor parts. Therefore, an increase of $\Psi \cdot \sigma_0$ will decrease the sensitivity of conductance measurements G_e.

Thus, all parts were cleaned with triton X100 (Sigma Chemical, USA) and flushed with de-ionized water before the assembly. The PEEK hollow cylinder was fixed onto an adhesion foil and stabilized from both sides. Then the tip of the PI foil was inserted into the tube manually. The process was observed visually by an assembly microscope (Olympus, SZX9). On both sidewalls of the PI foil, a thin layer of LOS 201 (Euro Lock) silicon glue was attached over a length of about 2.6 mm. Afterwards, the PI foil was inserted into the PEEK hollow cylinder. The silicone glue has a comparatively low viscosity and can therefore stick to the cylinder openings without filling the cylinder by capillary forces (wetting effects). The glue was also applied to the front part of the tube using a thin fiber to close the gap of the PI foil and the tube at the front part. The rear end of the sensor was also filled with silicon glue. After the curing of the adhesives, the sensor body was flushed with de-ionized water again before it was pushed into the membrane.

Shielded cable with an outer diameter of 1 mm and a length of 25 cm from Amgab EL AB (Sweden) was applied to make the connection between the sensor and the instruments. The wires were glued by conductive epoxy (CW2400, Chemtronics) to each side of the gold layers. The back part was then covered with Araldite standard epoxy resin to avoid any short circuit in case of any leakage of water.

2.1.5. Filling and sealing the sensor. The sensor was filled with de-ionized water through the filling holes at the rear end. The conductivity of the de-ionized water was about 2 μS cm^{-1} when measured by a conductometer (WTW Cond 340i). After the filling procedure was completed, the sensor was tested for electrical performance. When stable values were registered, the sensor was sealed by crimping a brass ring with an outer diameter of 1.3 mm at the rear end of the sensor.

2.2. Instrumentation

A lock-in amplifier (SR850, Stanford Research) was used for the testing of the sensors. We measured the admittance of the sensor by applying an amperometeric method with constant voltage and the corresponding current was then measured. The selected voltage was 50 mVrms to avoid noise and nonlinearity (Onaral and Schwan 1982). As the contribution error from the stray capacitance over 4 kHz is too large, and the electrode polarization contribution is mostly effective for frequencies under 100 Hz (Mirtaheri *et al* 2004), a frequency between 200 and 1000 Hz was found satisfactory. We chose a frequency of 700 Hz to avoid influence from both sources of errors. To make the impedance analysis of the sensor, we applied an impedance/gain-phase analyzer system (model 1260+1294 Solatron instruments). The sensor was connected to the instrument by shielded cables not longer than 50 cm and the impedance spectroscopy was done with an applied voltage of 50 mVrms.

2.3. Conditioning and measurements

2.3.1. Calibration and response. Three sensors were tested *in vitro* by submerging the sensor in a 20 ml container filled with 0.9% NaCl. The sensor response time and calibration were measured when the NaCl solution was bubbled with different CO_2 concentrations. A temperature sensor was placed separately in the solution to monitor the temperature changes. The concentrations for the gas tensions at 37 °C were 5, 10, 20 and 30 kPa, respectively. The measurements were tested with a blood gas machine (ABL 850, Radiometer AS, Denmark). The PCO_2 levels were corrected according to the measured temperature (Lide 2004). In addition to the solubility temperature correction, there is a 2%/°C temperature correction due to the conductivity temperature dependence (Foster and Schwan 1989).

For the response time testing, a 10 ml cylinder was filled with 4 ml NaCl and was then bubbled with N_2/CO_2 gas mixtures giving 10 and 30 kPa PCO_2 tension at 37 °C.

2.3.2. Temperature effect. The sensor was placed in a temperature-controlled incubator to test the effect of temperature on the baseline value of the sensor. The electrical impedance of the sensor as a function of frequency at the temperatures of 23–37 °C was measured.

2.3.3. Drift and pressure sensitivity. The sensor was tested for drift when submerged in a 0.9% NaCl solution for a period of 5 h. The test was performed at a temperature of 37 °C. The sensor values were monitored and logged with a 20 min interval.

For the pressure sensitivity, a 1 l glass cylinder with a small 3 mm diameter hole at the bottom was filled with 0.9% NaCl solution. The sensor was placed at the bottom of the glass cylinder. The sensor value was monitored while the NaCl solution ran out of the cylinder and consequently the pressure decreased. The testing was stopped when the level was about 0.1 l corresponding to 10 mbar.

2.3.4. Ex vivo measurements. In addition to the conductivity based sensor, a micro PCO_2 probe manufactured by Microelectrodes (MI 720, USA) was applied as a reference. The sensor's functionality was based on the Stow–Severinghaus principle (Stow *et al* 1957, Severinghaus and Brandley 1958). The sensor consisted of a glass pH probe, which was inserted into a plastic housing. At the tip of the plastic housing, a PTFE membrane with a thickness of 100 μm was placed. The outer diameter of the sensor was 3 mm and the length of the plastic housing was about 100 mm.

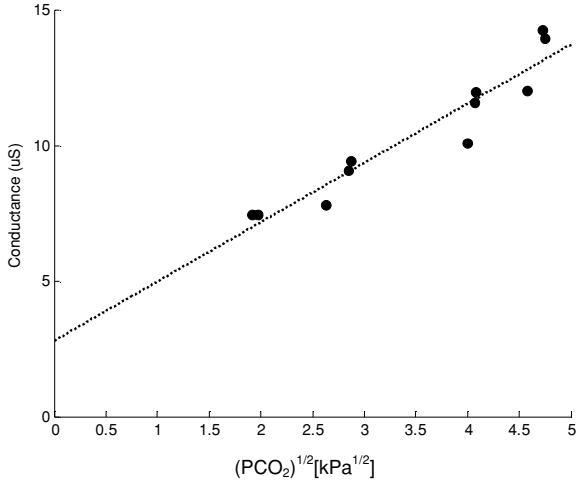

Figure 6. Calibration plot of the sensor showing measured conductance versus $(PCO_2)^{1/2}$.

The sensor was too large to penetrate the tissue, so we placed the sensor at the surface of the tissue. Since the membrane was placed at the tip of the sensor, there was problem with the effect from the ambient air that influenced the sensor measurement. To avoid the problem, we placed a silicone gasket at the tip of the probe to stabilize the sensor for surface measurements and prevent the ambient influence.

The micro PCO_2 probe as well as the conductivity based sensor was calibrated with 5, 10, 20, 30 kPa CO_2 tensions at 37 °C.

A small latissimus dorsi muscle flap (approximately 1 cm × 3 cm) was removed from an anesthetized pig that was used for another research study approved by the local ethical committee. In order to keep the muscle tissue moist, the muscle tissue and the sensors were placed into a test tube which then were covered by a plastic foil. The muscle temperature was kept at 37 °C by keeping the test tube in a thermostatic water bath adjusted to 37 °C.

3. Results and discussion

3.1. PCO_2 response

The calibration curve in figure 6 shows the measured response of the sensors as a function of the square root of PCO_2 tension. As predicted by theory, the PCO_2 response was proportional to the square root of PCO_2. A PCO_2 change of 3–20 kPa (corresponding to 1.7–4.5 $kPa^{1/2}$) had a conductivity change of 7–14 μS corresponding to 0.4 μS kPa^{-1}. The conductance of the sensor at zero kPa PCO_2 was formed by extrapolating the calibration curve and the result was about 2.8 μS. Assuming that the contributions from the reservoirs are minimal because of the selected geometry and only the channels are affecting the sensor total conductance, the expected conductance for the sensor would be about 1.2 μS when we have $\psi = 6\times10^{-3}$ m and the conductivity of water was 2 μS cm^{-1}. The sensor however did not show a sign of drift (cf 3.3), indicating the difference between the values is not caused by drifting. It would be for instance by ionic contamination of the chamber during the assembly or the mechanical behavior of the membrane.

The chemical reactions between water and carbon dioxide are so fast that its influence on the time response is negligible. As indicated previously, most of the time response should

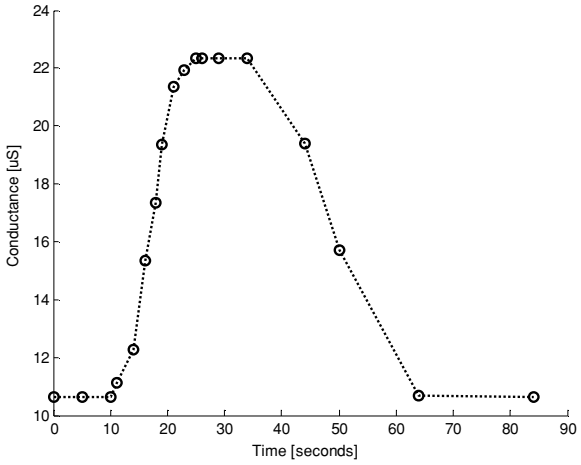

Figure 7. Typical response time with a step from 10 to 20 kPa CO_2 gas tensions.

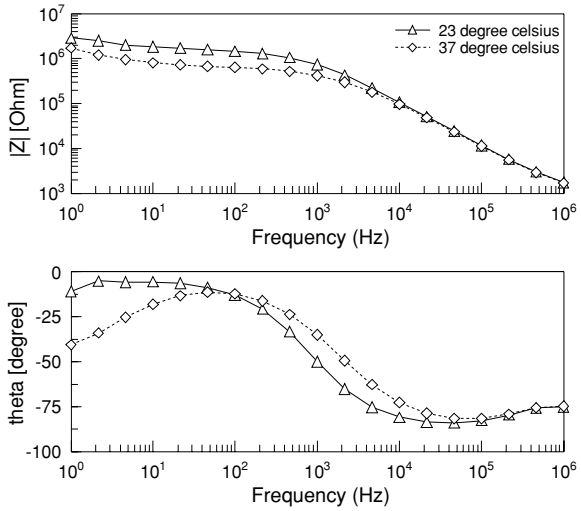

Figure 8. Measured complex impedance as a function of frequency with temperatures at 23 °C and 37 °C.

be due to the membrane for a miniaturized measurement cell (Mirtaheri *et al* 2004). The result of the response test is presented in figure 7. The response time was more rapid than the previous macro sensors; however, the characteristically fast response for the on-direction and a longer response for the off direction were reproducible. The typical quantitative values for on direction response time were between 5 and 10 s, while for the off-direction were between 30 and 35 s.

3.2. Temperature effect on baseline

The impedance value decreased with increased temperature as expected (figure 8). At frequencies above 3 kHz, the impedance was less affected by the temperature. This was probably due to the large effect of the stray capacitance at higher frequencies. Lis *et al* (1979)

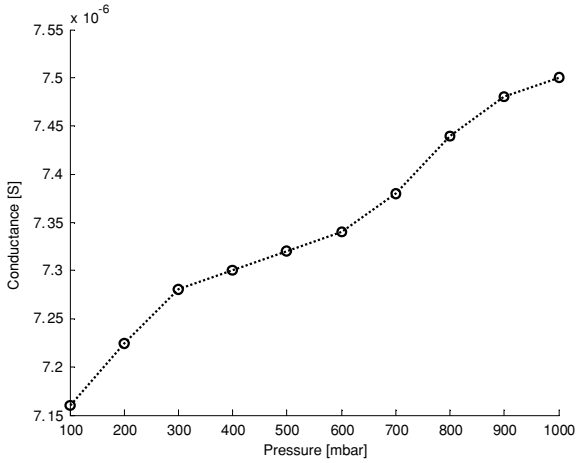

Figure 9. Conductance of the sensor as the function of external static pressure.

have suggested a 10%/K temperature contribution for the baseline. Our data at 700 Hz showed a 2.4%/°C temperature contribution which was more close to the 2%/°C value suggested by Foster and Schwan (1989).

3.3. Drifting and pressure

We found an average drifting of 0.4%/h of the baseline during 5 h testing (data not shown). The drifting reported by Lis *et al* (1979) was maximum 5%/h for their sensor realized with platinum electrodes and PTFE membrane. The reason for the drifting was not explained in their study; however, it might be due to an internal ion contamination from the parts or ionic contamination because of the poor sealing. Since we have particularly designed the sensor also with regard to the sealing, the sensor drift is minimal. The small changes of the total conductance were probably due to the mechanical changes in the membrane following its initial stretching.

Although the sensor was designed to be less pressure sensitive due to the walls between the channels, the sensor showed a response of 0.45 μS to the pressure changes between 10 and 100 mbar (figure 9). The conductance changed from 7.15 to 7.50 μS which corresponds to 1 kPa PCO_2 changes achieved by the calibration plot in figure 6. If the pressure in the air is about 0.3 kPa and assuming that all gases in the container are kept constant, the PCO_2 pressure will then increase tenfold and consequently the highest PCO_2 level would be 3 kPa. Since the measured pressure value is below the pressure expected from the calculation, we may conclude that the sensor is minimally pressure sensitive.

3.4. Ex vivo results

Figure 10 shows an example of *ex vivo* testing results of the conductivity based PCO_2 sensor compared to a Stow–Severinghaus sensor in a latissimus dorsi muscle. Since the Stow–Severinghaus probe was much larger and had to be placed on the surface of the tissue, the sensor was difficult to keep stable on the tissue and resulting in erratic measurements. However, both sensors showed a similar PCO_2 increase. Since the blood supply is cut-off in this *ex vivo* model, the PCO_2 will increase over time. Kvarstein *et al* (2004) reported that the

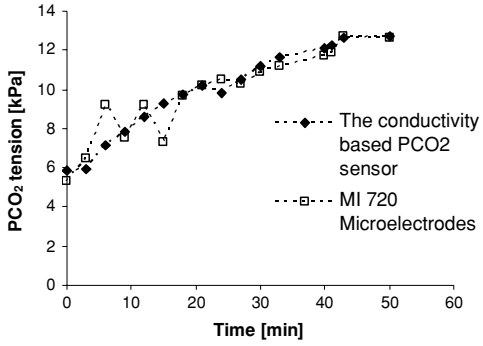

Figure 10. Example of an *ex vivo* testing with the conductivity based PCO_2 sensor compared to Stow–Severinghaus sensor.

PCO_2 level in the gluteal muscle tissues showed a baseline about 8.4 kPa, and after 30 min the value changed to 21.0 kPa *in vitro*. The results from our testing had an initial value of about 6.0 kPa and it changed to 10.0 kPa after 30 min measured by both sensors. The reason for the different measured values may be due to the leakage of gas from the test tube we applied. However, the conductivity based PCO_2 sensor showed similar results compared to the Stow–Severinghaus measurements in the muscle tissue.

4. Conclusion

The cylindrically shaped PCO_2 sensor based on conductometric measurement was redesigned to a miniaturized sensor design. The sensor manufacturing steps were specially considered in detail to achieve simple production. The sensor was able to measure PCO_2 changes and was stable *in vitro*. A much faster sensor was achieved by the small size and tiny polysiloxane membrane. The sensor measured an increase of PCO_2 in the *ex vivo* testing and the value of the PCO_2 increase was confirmed with Stow–Severinghaus sensor technology.

The information gained from this study has been used to manufacture an industrial PCO_2 version that can be applied to a clinical trial. The next version of such a sensor will be equipped with a temperature sensor to correct the measured PCO_2 values. The temperature sensor also gives the information about circulation of blood particularly if the sensor will monitor PCO_2 in extremities or superficial parts of the body.

Acknowledgments

We are grateful to Alertis Medical AS for the financial support. The authors would like to thank IMM (Institut für Mikrotechnik Mainz GmbH) for manufacturing the sensor parts, especially to Torsten Braune. Finally yet importantly, our special thanks to Sven Ivar Kristiansen at the instrument workshop at the Department of Physics, University of Oslo.

References

Arquint P 1994 Integrated blood gas sensor for PO_2, PCO_2 and pH based on silicon technology *PhD Thesis* University of Neuchatel

Foster K R and Schwan H P 1989 Dielectric properties of tissue and biological materials: a critical review *CRC Crit. Rev. Biomed. Eng.* **17** 25–104

Himpler H A, Brand S F and Brand M J D 1978 Conductimetric gas sensor for carbon dioxide *Anal. Chem.* **50** 1623–27

Grimnes S and Martinsen Ø G 2000 *Bioimpedance and Bioelectricity Basics* (New York: Academic)

Kvarstein G, Mirtaheri P and Tønnessen T I 2003 Detection of organ ischemia during hemorragic shock *Acta Anaesthesiol. Scand.* **47** 675–86

Kvarstein G, Mirtaheri P and Tønnessen T I 2004 Detection of ischemia by PCO_2 before ATP declines in skeletal muscle *Crit. Care Med.* **32** 232–7

Lide D R 2004 *CRC Handbook of Chemistry and Physics* www.hbcpnetbase.com.

Lis K *et al* 1979 A pCO_2 surface electrode working on the principle of electrical conductivity *Pflugers Arch.* **381** 289–91

Mirtaheri P *et al* 2004 A new biomedical sensor for measuring PCO_2 *Physiol. Meas.* **25** 421–36

Nunn J F 1993 *Nunn's Applied Respiratory Physiology* (Oxford: Butterworth & Heinemann)

Onaral B and Schwan H P 1982 Linear and nonlinear properties of platinum electrode polarization. Part1: Frequency dependence at very low frequencies *Med. Biol. Eng. Comput.* **20** 229–306

Severinghaus J W and Brandley F 1958 Electrodes for blood PO_2 and PCO_2 determination *J. Appl. Physiol.* **13** 515–7

Schlichtig R and Bowles S A 1994 Distinguishing between aerobic and anaerobic appearance of dissolved CO_2 in intestine during low flow *J. Appl. Physiol.* **76** 2443–51

Schwan H 1968 Electrode polarization impedance and measurements in biological materials *Ann. New York Acad. Sci.* **148** 191–209

Schwan H P and Ferris C D 1963 Four-electrode null technique for impedance measurements with high resolution *Rev. Sci. Instrum.* **39** 481–3

Stow R W, Baer R F and Randall B F 1957 Rapid measurement of the tension of carbon dioxide in blood *Arch. Phys. Med. Rehabil.* **7** 646–50

Tønnessen T I 1997 Biological basis for PCO_2 as a detector of ischemia (review) *Acta Anaesthesiol. Scand.* **41** 659–69

Tønnessen T I and Kvarstein G 1996 PCO_2 electrodes at the surface of the kidney detect ischemia *Acta Anaesthesiol. Scand.* **40** 510–9